TECHNICAL REPORT R-105

SPUTTERING OF METALS BY MASS-ANALYZED N_2^+ AND N^+

By MICHEL BADER, FRED C. WITTEBORN, and THOMAS W. SNOUSE

Ames Research Center
Moffett Field, Calif.

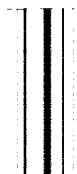

TECHNICAL REPORT R–105

SPUTTERING OF METALS BY MASS-ANALYZED N_2^+ AND N^+

By Michel Bader, Fred C. Witteborn, and Thomas W. Snouse

SUMMARY

Low-energy sputtering studies were conducted with the help of a specially designed ion accelerator. A high-intensity rf ion source was developed for application to relatively low-yield experiments requiring good energy resolution in the 0 to 8 kev energy range. This source, used in conjunction with electrostatic acceleration and focusing, and magnetic mass analysis, has produced beams of 200 to 500 μa of N^+ or N_2^+ ions with energy-dispersion half-widths of about 20 ev.

The sputtering yields of five metals (Cu, Ni, Fe, Mo, *and* W) *were investigated over the available energy range at normal and 45° incidence. The yields obtained are generally similar to those reported in the literature for different bombarding ions; they increase rapidly with energy from a threshold below 25 ev and reach a plateau around 3 kev. Yields at 45° incidence are higher than at normal incidence, by about 25 percent for* Cu, *and by 50 to 100 percent for* Ni, Fe, Mo, *and* W. *The effect of 2 N^+ ions tends to be smaller than that of an N_2^+ ion with the same total kinetic energy at low energies, but equal to or greater than the N_2^+ effect at higher energies. Significant yields have been detected at energies often quoted as threshold or below threshold (around 25 ev).*

The data do not correlate into consistent patterns through the use of the principal known parameters of the sputtering process: ion-lattice and lattice-lattice energy and momentum transfers, heats of sublimation, and types of crystal structure. It is concluded that the process cannot be described adequately as a succession of binary collisions.

INTRODUCTION

The erosion of metallic surfaces under positive ion bombardment was first detected (over 100 years ago) in glow discharges, which explains its early designation, "cathode sputtering." Extensive experimental and theoretical investigations of this process were carried out, starting around 1920. Studies of cathode sputtering soon tapered off, however, and were not vigorously revived until around 1950, when interest was kindled anew by the emergence of applications outside the vacuum tube technology field. The phenomenon then came to be more generally denoted simply "sputtering." The newer questions were raised as a consequence of outer atmosphere and space research, and they concern the gross, or engineering, behavior of surfaces subjected to atomic-size particle bombardment in the space environment. Indeed, erosion rates in a given environment determine the useful lifetime of certain critical surfaces; thin films may altogether disappear, or desired optical and radiative properties may be severely altered. In addition, an interesting recent development has been a return of attention to cathode sputtering as such, in connection with studies of ion propulsion devices—again because of the useful lifetime problem.

All bombarding particles and target materials are of theoretical interest, as the physical processes involved in sputtering are not well understood; differences in behavior between the many possible particle-target combinations should yield useful clues and must, of course, be accounted for by proposed theories. An understanding of sputtering would also shed light on an important associated problem, that of predicting the modes of reflection of the impinging particles or their accommodation coefficients.

The particles and associated bombarding energies of immediate engineering interest are the ions used in propulsion devices, at kev energies; the

particles of the earth's and other planets' atmospheres, impinging on vehicle structures with energies of a few ev (corresponding to their velocity relative to the vehicle); and interplanetary or interstellar particles with energies ranging up to billions of electron-volts. The higher energy particles do not, however, contribute to sputtering; as their kinetic energies become higher, the bombarding particles penetrate deeper into the target material and their effect shifts from sputtering to radiation damage. The number of target atoms ejected per incident particle, known as the sputtering ratio or yield, rises from very low values at electron-volt energies, reaches a plateau at a few kev, then diminishes again as effects of bombardment become internal to the target. The energies at the turning points depend on the bombarding particle size, as this determines penetrating ability (compare, e.g., A^+, He^+, and D^+ data in ref. 1). Practically, then, the energy range of interest for sputtering by all particles is from a few ev up to about 200 kev.

All the early experimental studies were performed in glow discharges of noble gases. The large bombarding current densities so obtainable are a significant advantage in producing measurable effects in reasonable lengths of time. In addition, the ion bombardment rate can usually be made large compared to the bombardment rate of residual gases, so that the target surfaces can be considered relatively clean. The background pressures, however, are of the order of 10^{-3} mm Hg or more, in which region there exist problems of (a) scattering of the incident ions (noncontrol of angle of incidence), (b) charge exchange and neutral bombardment (loss of knowledge of total bombarding rate), and (c) back-scatter of sputtered atoms to the target. Further disadvantages of glow discharges are: secondary electron emission from the target is difficult to suppress, so that an additional uncertainty in bombarding rate is introduced; mass analysis of the incident beam is not possible, so that the method is effectively limited to bombarding ions of monatomic elements; and the bombarding energy is difficult to control and measure. Some of these limitations can be at least partially circumvented, and particularly ingenious techniques have been devised in the last decade by Wehner, who has used principally mercury ions (see ref. 2, in which Wehner gives a comprehensive review of sputtering studies to 1955).

More recent experimental work has shown a trend toward ion-beam techniques, using accelerators and mass separators in which the beam energy, composition, and angle of incidence can easily be controlled, secondary electrons can be suppressed, and high vacua can be maintained. Large beam intensities with good energy resolution are, however, hard to obtain at low energies, so that work has generally been done from a few kev up (refs. 1, 3, 4, 5, and 6). At lower energies, some data have been obtained by using detection techniques dependent on unusual target material properties (such as surface ionization or radioactivity) and hence these techniques are of limited applicability (refs. 3, 5, and 7). Finally, considerable additional and increasingly refined work has been performed by Wehner and his coworkers (refs. 8 through 14) in glow discharges, yielding data at low energies for noble gas and mercury ions bombarding many metallic surfaces and the semiconductor germanium.

Two basic concepts were early set forth in building theories of sputtering (see Wehner's review article, ref. 2): momentum exchange between the incident and the lattice particles, and local dissipation of the incident energy leading to surface evaporation. Later theories have essentially refined the basic ideas by introducing the statistics of many collision processes and the lattice constants of the target materials. Keywell (ref. 15) and, with additional attention to individual collision details, Harrison (refs. 16 and 17) have introduced parameters and used mathematical formulations which are analogous to those of the theory of neutron diffusion and cooling in solids. Henschke (ref. 18) and Langberg (ref. 19) proposed a series of binary collisions in which energy dissipated in the lattice is taken into account. Henschke uses the elementary concept of a "coefficient of restitution," while Langberg uses a more sophisticated model for the interactions and allows rebounding lattice atoms as well as the incident particle to contribute to the sputtering. Presently available data are not sufficiently detailed and accurate to differentiate between competing theories. It is generally expected, however, that energy and diffusion concepts will be more valid at high energies, while

momentum and binary collision concepts may explain low energy sputtering.

The theoretical interest, together with the immediate space research application, prompted the investigation, at the Ames Research Center, of the possibility of extending ion accelerator techniques to low energies. A suitable ion source and accelerator system were developed and constructed for Ames by the Stanford Research Institute under the direction of Drs. C. J. Cook, J. R. Peterson, and O. Heinz. The apparatus, as modified at Ames for improved performance, is presently yielding 100 to 500 μa of analyzed positive ion beam on a 1 cm^2 target area with good energy resolution down to about 250 ev.

The construction, performance, and probable limitations of the Ames low-energy ion accelerator will be discussed in the next section of this report. We shall then present the sputtering yield curves obtained to date with separated N_2^+ and N^+ beams and discuss their probable significance and implications.

APPARATUS AND PROCEDURE

THE 8-KV ACCELERATOR

A general view of the 8-kv ion accelerator used for the studies herein reported is shown in figure 1, and schematic diagrams are given in figures 2 and 3. The ions are extracted from an rf source, electrostatically focused into a 90° magnetic analyzer, then electrostatically refocused into the target chamber.

The main distinguishing feature of the apparatus is the ion extraction mechanism. The ions are formed by inductively coupling a 25 Mcps electric field to a low-pressure (10^{-3} mm Hg) gas which is contained in a Pyrex jug (approximately 2-inch diameter by 5-inch height). The jug is mounted on an insulated platform, normally maintained at

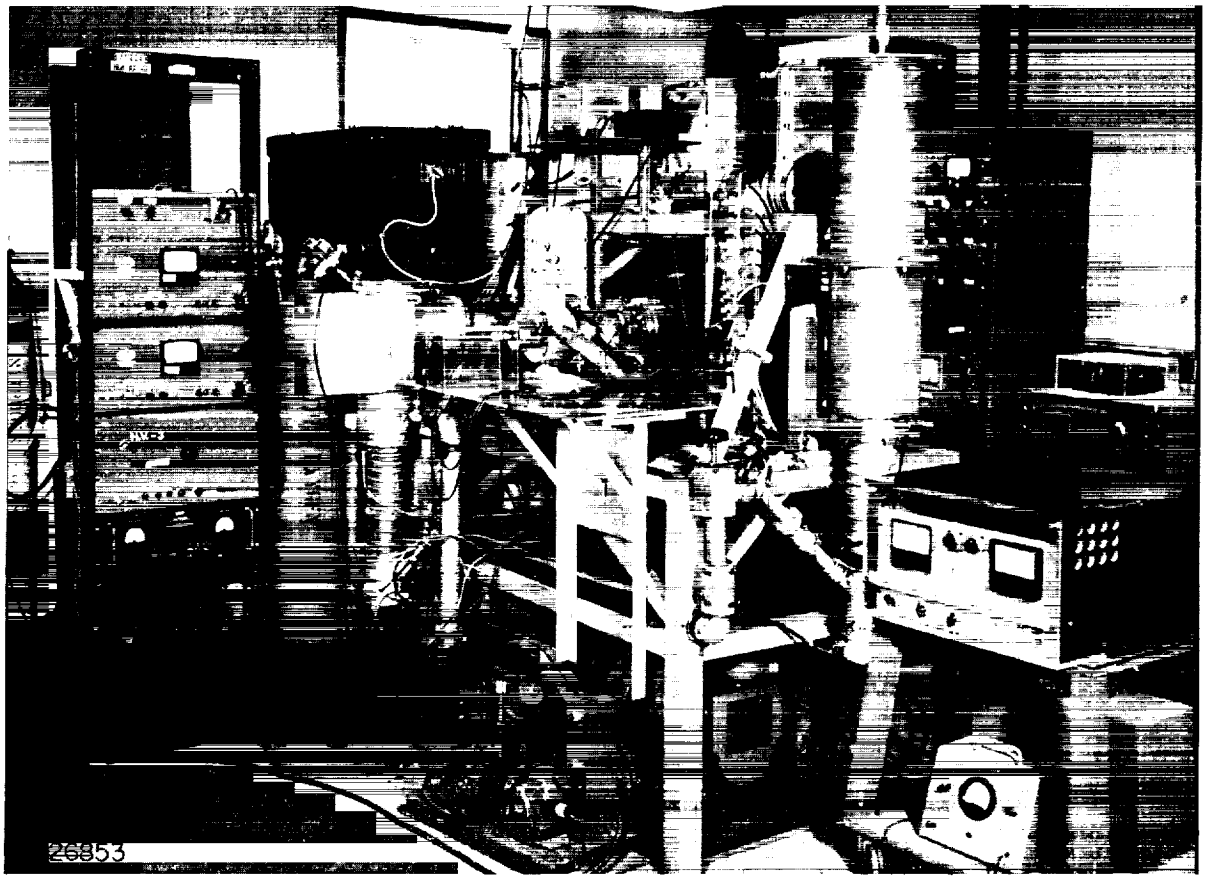

FIGURE 1.—General view of 8 kv ion accelerator.

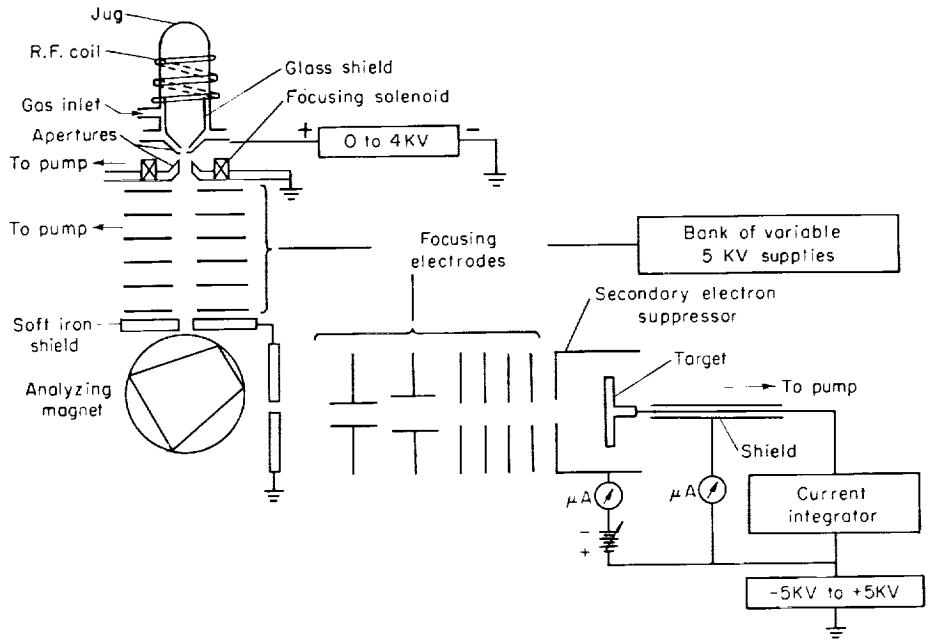

FIGURE 2. Schematic diagram of 8 kv ion accelerator.

a dc potential of 3600 v (see fig. 2). The extraction aperture is a 0.375-inch hole in the platform, glass-shielded so that only a small metallic rim is exposed to the plasma. Ions are then emitted from the concave plasma sheath at the first aperture under the influence of the potential drop to the grounded second aperture located about 0.25 inch below the first (fig. 2; see also ref. 20). An axial magnetic field is used between the two apertures to vary the ion density at the sheath and immediately below.

The plasma itself is thus at a uniform dc potential. This is in contrast to the more conventional operation of rf sources, in which a probe placed at the top of the jug to collect residual electrons subjects the plasma to a dc

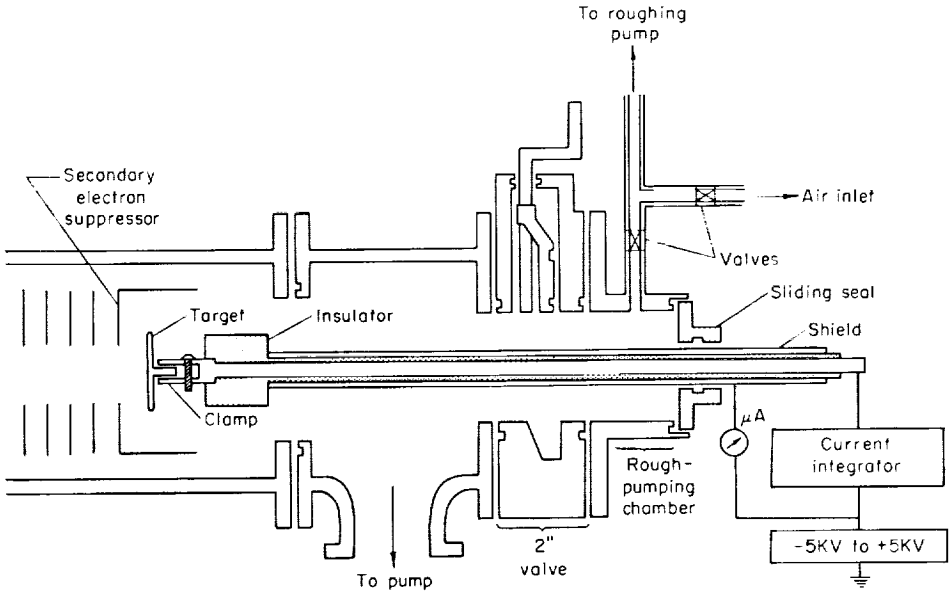

FIGURE 3. Schematic diagram of the target assembly.

drop, so that the ions are created at different potential levels. Aperture extraction results in a total energy dispersion as low as 10 ev and ranging up to 100 ev, depending primarily on rf power level. The total beam energy was found to be unexpectedly high, ranging from 100 to 300 ev above the extraction drop. The high plasma potential can probably be accounted for by the rf acceleration of a small number of plasma electrons to high energies (ref. 20). No correlation was found between excess energy and energy dispersion, and a satisactory explanation for the observed dispersions has not been found. The beam characteristics are, however, reproducible for given sets of values of jug pressure, rf power, extraction voltage, and extraction magnet current.

The extracted beam passes through an electrostatic lens system whose configuration, possibly not fully optimized, was determined experimentally. Ionic species are then separated by a 90° magnetic analyzer which is followed by a second electrostatic lens system (fig. 2) and by the target assembly (figs. 2, 3, and 4). Separate variable ±5 kv supplies and micro-ammeters individually control and monitor the lens and suppressor electrodes. It is thus possible to make sure that a negligible amount of beam strikes the electrodes, especially those immediately ahead of the target, and that proper secondary electron suppression is obtained at the target. The suppressor construction made use of a wire-grid configuration (fig. 4) in order to minimize the possibility of reflection of sputtered atoms back to the target. Hence, sputtering of electrode material onto the target and secondary emission from the suppressor to the target can, in general, be held to a negligible level.

Beam energy variation is obtained by changing the extraction and target voltages. The correction for the excess energy of the source is obtained for any given set of operating parameters (source pressure, etc.) by making retarding potential measurements at the target. A typical plot

FIGURE 4.—Photograph showing, from left to right: (1) last focusing stages of electrostatic lens; (2) wire grid secondary electron suppressor; and (3) target (mounted at 45° to the beam axis).

of target current as a function of target voltage relative to extraction voltage is shown in figure 5.

The energy dispersion in the beam can be kept below 40 ev (total width at half maximum, see fig. 5) and is nearly symmetrical. Since the yield curves are essentially linear over such a small range, no correction need be made to the yield values on account of dispersion. This is not true at beam energies below about 250 ev, however, and one must either (a) introduce electrostatic beam analysis at a sacrifice in beam currents, or (b) determine accurately the energy distribution in the beam and correct mathematically for the fact that the measured yield at a given voltage setting is an integrated value. Data for copper and nickel were obtained by this last technique down to 20 ev at normal incidence.

Because of extraction characteristics and space charge blow-up of the beam, it was found preferable to keep the extraction aperture between 1 and 4 kv (typically 3.6 kv). The relatively large retarding fields needed near the target for obtaining low-energy bombardment then tend to introduce an angular spread of the beam, particularly when the target plane is not normal to the beam. For bombarding energies down to 250 ev it was found possible to control the beam angle of incidence to within $\pm 5°$ by careful focusing. Since the suppressor is typically 100 v negative with respect to the target, larger angular uncertainties are present at beam energies under 250 ev.

The source pressure is typically 1×10^{-3} mm Hg. Differential pumping at the source and pumping behind the target (figs. 2 and 3) keeps

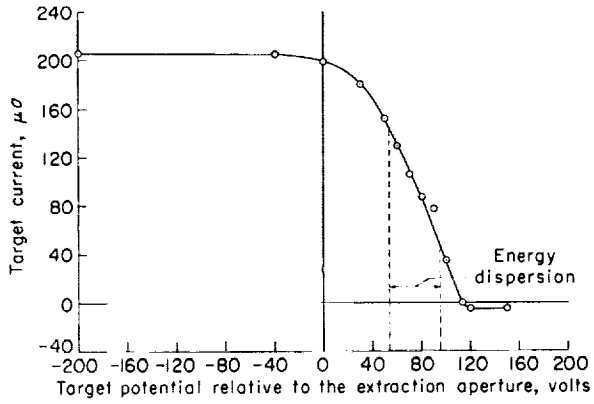

FIGURE 5.—Target current as a function of the target potential relative to the extraction aperture.

the operating pressure below 1×10^{-5} mm Hg at the target (beam current ≈ 500 μa). Three 4-inch oil-diffusion pumps with individual copper baffles and liquid nitrogen traps are used. Spectroscopic examinations of the targets failed to reveal the presence of surface contaminations, in particular hydrocarbons.

Under conditions controlled as described above, the accelerator presently delivers 200 to 500 μa of N_2^+ to a 1 cm^2 spot on the target at energies of 250 ev to 8 kev with a total energy dispersion of 10 to 40 ev. Corresponding N^+ currents range from 50 to 200 μa. Preliminary data indicate that no significant changes in performance are to be expected for operation with other ions. A minor exception is that the jug pressure must be kept higher for lighter gases ($\sim 5 \times 10^{-3}$ mm Hg for H^2), so that additional pumping capacity may have to be provided to maintain an adequate vacuum in the rest of the system.

TEST PROCEDURE

Sputtering yields in atoms per ion were computed from the measured weight losses of targets subjected to a known amount of bombardment. Targets were machined in the shape of (or attached to) 1-inch-diameter disks, ⅛ inch thick, with a mounting and handling knob on one face (fig. 3). Targets were cleaned with ordinary solvents, such as acetone, and kept in a desiccator until mounted, and then quickly introduced into the rough-pumping chamber. The 2-inch gate valve could be opened and the target pushed into position behind the suppressor electrode within two minutes. This procedure was reversed for removing the targets after bombardment. Except for the small roughing chamber, all parts of the apparatus could thus be constantly kept under high vacuum.

The targets were weighed on a Mettler Type M5 microbalance after stays of 1 to 4 hours in the desiccator (to ensure reproducibility of possible adsorptions). Targets were put through the above complete procedure, except for bombardment, and found to weigh the same before and after to within the weighing accuracy of ± 5 μg (the balance is capable of more accuracy, but this requires a degree of air conditioning which was not available at the time of these measurements). The sputtering weight losses typically ranged from 500 to 2,000 μg, though a few data points were obtained

i

n the 100 to 500 μg range because of time limitations (bombardment times ranged from 30 min to 4 hrs). The number of atomic layers removed ranged from 250 to 23,000. Visible roughening of the surfaces occurred, and as one might expect, no difference in yield was observed between first run and resputtered targets. The surfaces were, however, repolished when enough sputtering had occurred to introduce an uncertainty in macroscopic angle of incidence.

The total charge delivered to the target (0.5 to 4 coulombs) was measured to ±1 percent by an El Dorado Model CI–100 current integrator. The instrument calibration was periodically checked with standard cells and capacitors, and found constant to better than 0.5 percent.

RESULTS

A sputtering yield curve for Cu bombarded at normal incidence by A^+ ions (fig. 6) was obtained to offer a comparison with available data from other observers (including representative early data, refs. 21 and 22). This seemed desirable since no data were found for such a comparison for nitrogen-ion bombardment.

A special effort was made to obtain data for copper and nickel at very low bombarding energies. Results for normally incident N_2^+ and N^+ ions with 20 to 900 ev are given in figure 7. The data have been corrected for energy dispersion in the beam with the help of retarding potential curves (fig. 5). Yields are still appreciable, of the order of 0.1 atom/ion, at 25 ev.

The values obtained for the sputtering yields of Cu, Ni, Fe, Mo, and W are given graphically

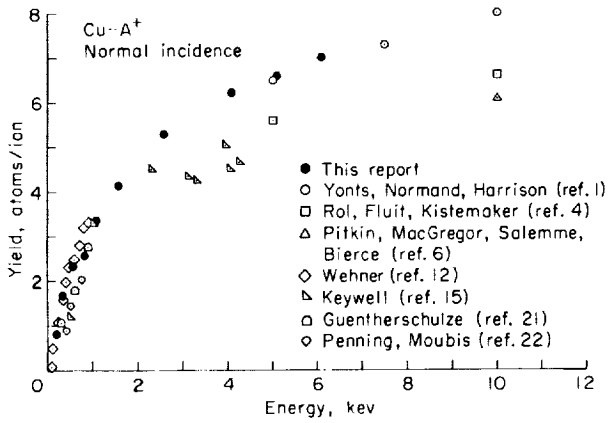

FIGURE 6.—Sputtering yield of copper bombarded by A^+ ions as a function of ion energy; normal incidence.

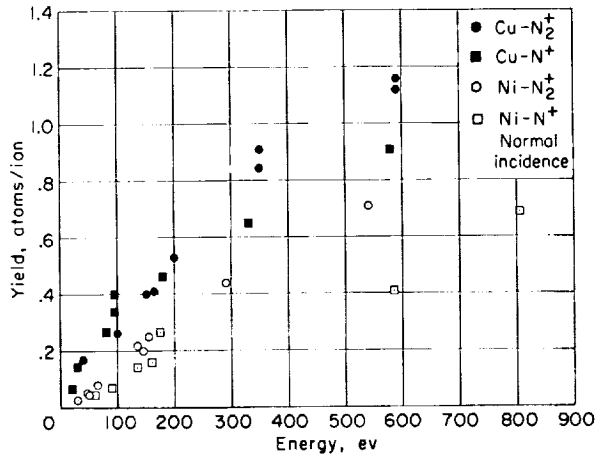

FIGURE 7. Sputtering yields of copper and nickel bombarded by N^+ and by N_2^+ ions at energies below 900 ev; normal incidence.

as a function of bombarding energy (250 ev to 8 kev), bombarding ion (N_2^+ and N^+), and angle of incidence (normal and 45°) in figures 8 through 12. The yields increase rapidly with energy from a low value around 25 ev and tend to level off above 3 kev. Yields at 45° incidence are higher than at normal incidence, by about 25 percent for Cu, and by 50 to 100 percent for Ni, Fe, Mo, and W. The effect of 2 N^+ ions tends to be smaller than that of an N_2^+ ion with the same total kinetic energy at low energies, but equal to or greater than the N_2^+ effect at higher energies (figs. 13 and 14).

Sputtering yields were found to be about 10 percent higher at a target chamber pressure of 6×10^{-6} than at 6×10^{-5} mm Hg. No dependence of yields on target temperature was found between 40° and 120° C, except for a drop of about 20 percent in Fe yields between 80° and 40° C.

DISCUSSION

PRINCIPAL YIELD CURVES

Comparison with other data.—Our results for copper are plotted in figures 7 and 8 together with the data obtained in Amsterdam by Rol, Fluit, and Kistemaker (ref. 4) where the energy ranges overlap. The discrepancy between these two sets of data is outside our probable experimental error, and for argon bombardment a discrepancy of the same magnitude exists between the Amsterdam results and ours (fig. 6). The Cu–A^+ yields which were obtained at Oak Ridge by Yonts,

Normand, and Harrison (ref. 1) agree very closely with ours (fig. 6). The Oak Ridge group noted the discrepancy with the Amsterdam results and attributed it to a pressure dependence of sputtering; in effect they surmised that the vacuum in the Amsterdam isotope separator was not as high as that obtainable in the Oak Ridge calutron. Our own evidence tends to support this view, as will be shown later in the discussion of pressure effects. Similar conclusions can be reached in regard to the yield values obtained by Pitkin, MacGregor, Salemme and Bierce (ref. 6) in the 10 to 40 kev range; their values were obtained at test chamber pressures above 10^{-3} mm Hg, and are low compared to the Oak Ridge values obtained at pressures of about 4×10^{-5} mm Hg.

Cu and Ni yields.—Copper and nickel both have face-centered cubic lattices, and their atomic weights are similar (Cu, 63.54; Ni, 58.71). The energy-transfer characteristics from the ion to the lattice and within the lattice are thus expected to be similar for any simple mechanical model, and the yield curves should exhibit similar characteristics. For example, the slight downward trend of the normal incidence Cu–N^+ yield above about 6 kev (fig. 8(a)) is also observed for Ni–N^+ (fig. 9(a)). Many inconsistencies between the data and predictions of mechanical models are present, however, and will be made apparent in further discussion.

The generally higher sputtering rate of copper can be qualitatively accounted for by its lower atomic heat of sublimation (Cu, 3.557 ev; Ni, 4.413 ev). Preliminary measurements indicate, however, that aluminum, also an fcc metal, has a lower sputtering rate than either nickel or copper

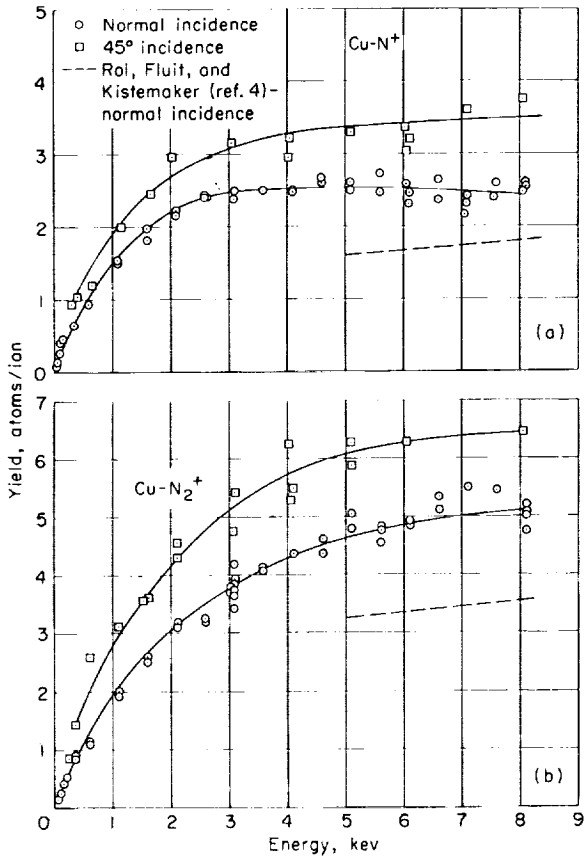

(a) Cu—N^+
(b) Cu—N_2^+

FIGURE 8. Sputtering yield of copper bombarded by N^+ and by N_2^+ ions as a function of ion energy; normal and 45° incidences.

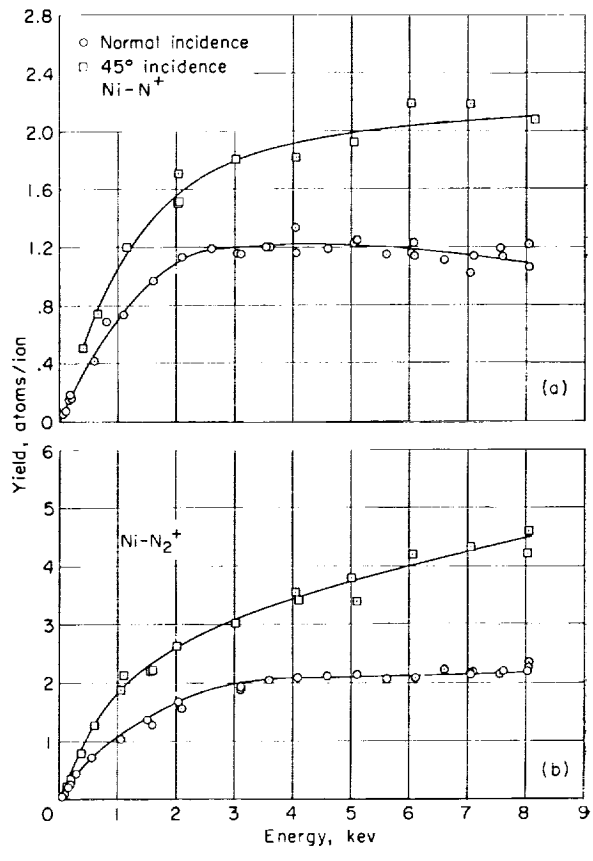

(a) Ni—N^+
(b) Ni—N_2^+

FIGURE 9. Sputtering yield of nickel bombarded by N^+ and by N_2^+ ions as a function of ion energy; normal and 45° incidences.

in spite of its lower atomic heat of sublimation, 3.252 ev. The relative importance of the incident particle and of displaced lattice particles in the sputtering process has not been definitely established, but it is worth noting that the mechanical ion-lattice energy transfer is more efficient from nitrogen to aluminum (at. wt. 26.98) than to copper or nickel. Note also that aluminum has a relatively low sputtering yield under Hg^+ bombardment (ref. 9), in which case the ion-lattice energy transfer is less efficient than that for Cu–Hg^+ or Ni–Hg^+.

Comparison of normal and 45° yields.—An important inconsistency with the anticipated similarity between Cu and Ni yield curves is the following. The 45° Cu yields are consistently 20 to 30 percent above those at normal incidence, while the difference between 45° and normal incidence Ni yields increases noticeably with energy, reaching about 110 percent of the normal yield at 8 kev. For Hg^+ bombardment (ref. 12), generally smaller angular dependencies have also been found for Cu and the noble metals, Ag, Pt, and Au, than for Ni (all these metals are fcc). This is not presently understood: One might expect the electronic configuration of the target atoms to affect the sputtering rates, but not to affect the dependence of these rates on the angle of incidence of the bombarding ion. This latter effect should depend primarily on the geometric parameters, crystal structure and crystal orientation (random, in the experiments reported).

The yield curves of the body-centered cubic metals, iron, molybdenum, and tungsten, are shown in figures 10 through 12. The 45° yields are 100 to 125 percent higher than those at normal incidence for Fe–N_2^+ and Mo–N_2^+, and 50 to 75 percent for W–N_2^+. Similar numbers for N^+ bombardment are not as high: 30 to 50 percent for Fe–N^+ and W–N^+, and 80 to 100 percent for Mo–N^+. Wehner, using Hg^+ bombardment (ref.

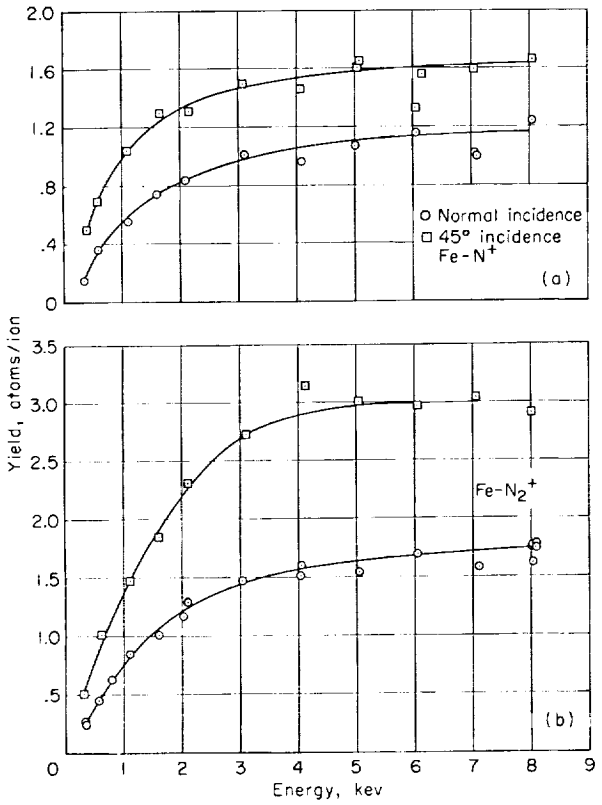

(a) Fe–N^+
(b) Fe–N_2^+

FIGURE 10. Sputtering yield of iron bombarded by N^+ and by N_2^+ ions as a function of ion energy; normal and 45° incidences.

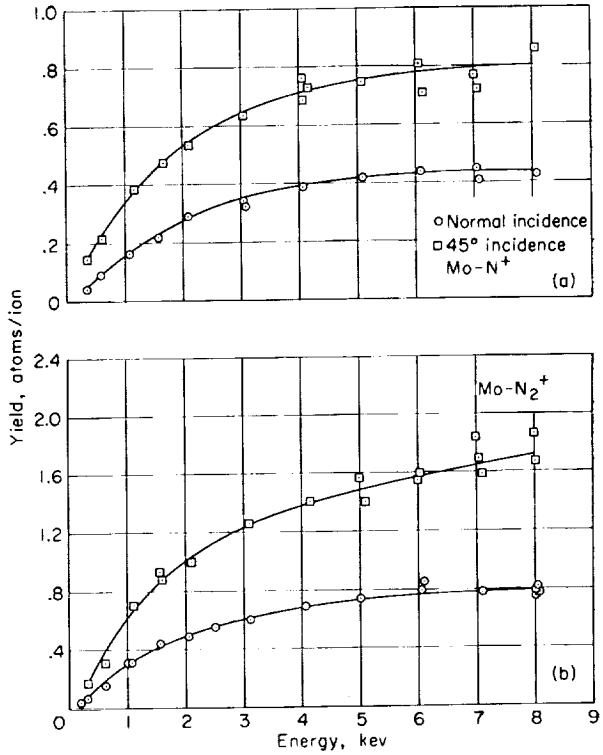

(a) Mo–N^+
(b) Mo–N_2^+

FIGURE 11. Sputtering yield of molybdenum bombarded by N^+ and by N_2^+ ions as a function of ion energy; normal and 45° incidences.

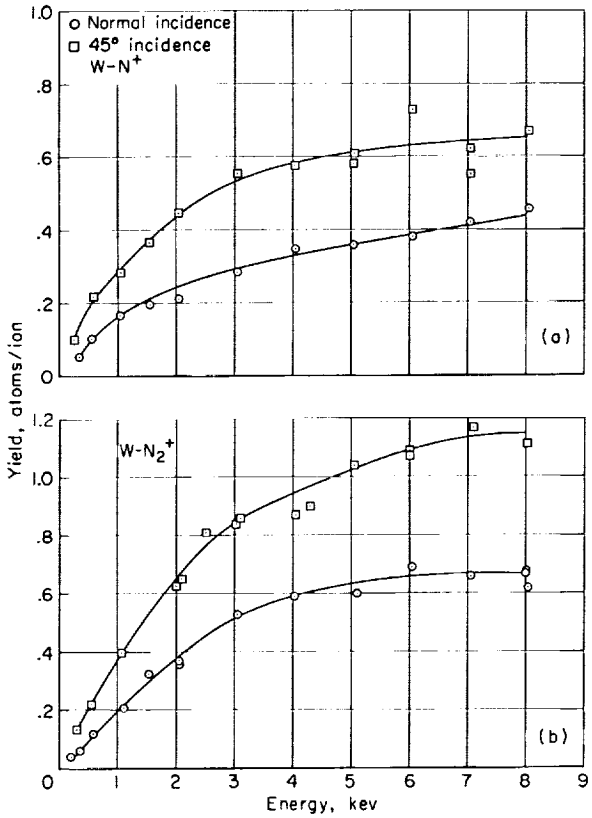

(a) W N^+
(b) W N_2^+

FIGURE 12. Sputtering yield of tungsten bombarded by N^+ and by N_2^+ ions as a function of ion energy; normal and 45° incidences.

12), also found the angular dependence of sputtering more pronounced for Fe and Mo and least for Cu. (We recall that our differences for Cu were 20 to 30 percent.) Furthermore, Wehner reported much larger ratios of 45° to normal yields than those reported here; the Mo–Hg difference at 800 ev, for example, is about 1400 percent. This is in qualitative agreement with our observation that the 45° to normal yield ratio increases with the mass of the bombarding ion.

Comparison of N^+ and N_2^+ yields.—Further examination of the data, however, reveals some serious difficulties in the comparison of N^+ with N_2^+ yields. The impinging ion is neutralized on impact, and the neutralization energy, 15.5 ev, is negligible compared to the bombarding energy so that sputtering can be assumed to be charge-independent. Since, in addition, the dissociation energy of N_2 is 9.76 ev, one would expect, in the energy range under consideration, the N_2 molecule to break up on impact into two atoms, of about equal energy, which then might act independently. If this were indeed the case, sputtering by N_2^+ should be equivalent to sputtering by $2N^+$ with the same total energy, and there should be no difference in the 45° to normal yield ratios of N_2^+ and N^+.

The total normal incidence yield for $2N^+$ ions, each with 1/2 the energy of an N_2^+ ion, is plotted together with the data for N_2^+ in figure 13. The agreement between N_2^+ and $2N^+$ yields is excellent for the fcc metals, Cu and Ni, although there seems to be a slight tendency for Ni–$2N^+$ to be too high at high energies. This may not be significant, in view of the maximum in the Ni–N^+ yield curve; unfortunately, Ni–N_2^+ data with which to continue the comparison above 8 kev are not available.

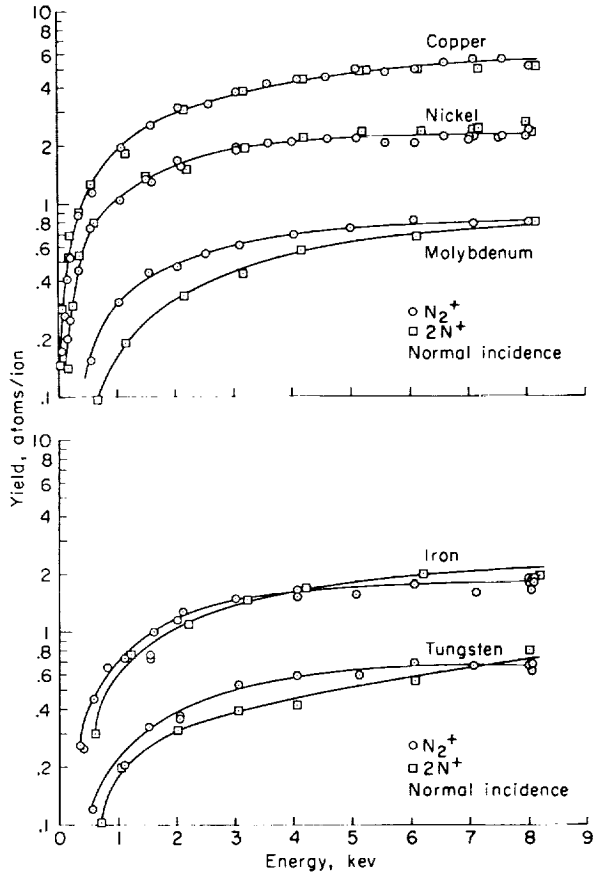

FIGURE 13. Comparison between the yields resulting from bombardment by N_2^+ and those from 2 N^+ (each N^+ with ½ the N_2^+ energy); normal incidence.

The agreement is not at all as good in the cases of the bcc metals, Mo, Fe, and W. Here the $2N^+$ curves lie below the corresponding N_2^+ curves at low energies, then cross over to the high side at the high-energy end. This behavior has also been noted by Gronlund and Moore (ref. 5) who bombarded silver (an fcc metal) with various isotopes of atomic and molecular hydrogen.

Three possible explanations for these discrepancies are the following. First, the assumption of charge-independence of sputtering may not be valid. (The possible significance of the electronic configuration of the target atoms has already been noted in connection with 45° to normal incidence yield ratios.)

Second, it has been suggested that the initial ion-target collision might play the dominating role in the sputtering process, and since N_2^+ can transfer more energy to a target atom in one collision than can N^+, the N_2^+ yields should be higher. It must be pointed out, however, that $2N^+$ can transfer more energy than N_2^+, if one assumes a classical interaction. Furthermore, the initial momentum transferred is directed into the target, and only reflected momentum can cause sputtering. Energy and momentum-transfer theories have been checked for many metal-ion combinations by plotting sputtering yields versus energies normalized by maximum transferable energy factors, momentum transfer factors, and combinations of these with atomic heats of sublimation (refs. 9, 15, and 19); no valid correlations were found. Such plots similarly do not bring out correlations between N^+ and N_2^+ yields.

A third possible explanation for the $2N^+$ versus N_2^+ discrepancy has been offered. The increase in yields at oblique incidence has been ascribed to a smaller depth of penetration of the particle into the target. If this is so, it would appear that the incident particle retains its initial direction over a significant distance. This, however, would not be true of the atoms from normally incident N_2^+; these atoms probably have an oblique initial direction of motion, and hence, could cause more sputtering than two normally incident N^+ ions.

This last hypothesis can be investigated further by plotting comparison curves ($2N^+$ and N_2^+) for 45° incidence data; it seems reasonable to assume that the initial motion of the atoms from 45° incident N_2^+ is on the average at 45°, so that the comparison may have more validity than that for normal incidence. The 45° plots, shown in figure 14, exhibit two surprising features: First, the low energy discrepancies are emphasized, rather than reduced, and even appear in copper and nickel; the one exception is tungsten, for which the 45° $2N^+$ and N_2^+ curves coalesce to within experimental scatter. Second, the $2N^+$ curves no longer cross to the high side of the N_2^+ curves at high energies. These observations are in direct contradiction to our expectations, and no satisfactory explanations have been found.

The threshold region.—We conclude the discussion of the yield curves with some remarks on sputtering in the threshold region. The following definitions are important for this discussion. The threshold energy is, of course, the intercept of the yield curve with the energy axis (it is a difficult quantity to determine experimentally).

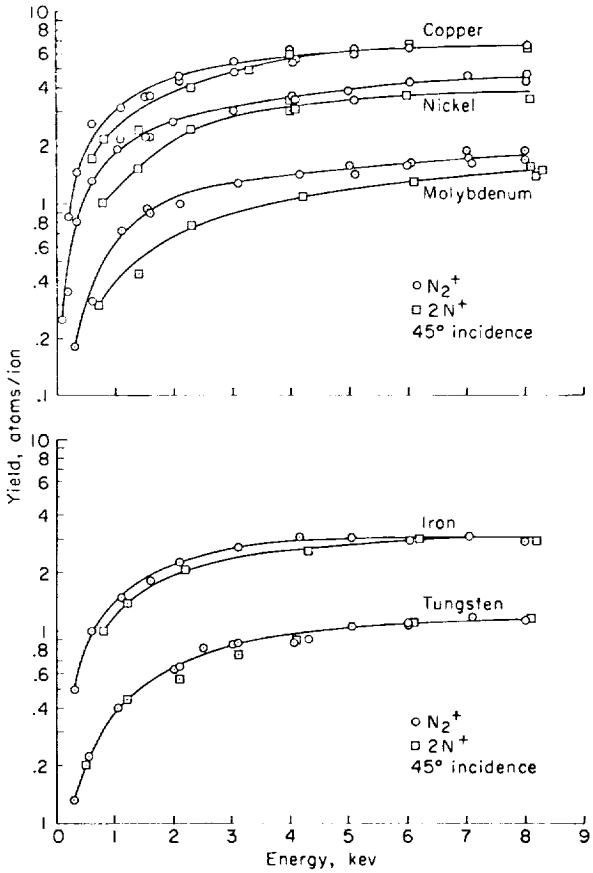

FIGURE 14.—Comparison between the yields resulting from bombardment by N_2^+ and those from 2 N^+ (each N^+ with ½ the N_2^+ energy); 45° incidence.

Another energy has been defined, the "cut-in" energy, which is the intercept of the extrapolated linear part of the yield curve with the energy axis. (Yields tend to be linear functions of energy in the 100 to 500 ev range.)

Langberg (ref. 19) has given one of the best theoretical discussions of these energies. He takes into account the atomic heat of sublimation of the metals, the numbers and types of bonds holding surface atoms, and the energy transferable from the ion to the lattice in the first collision. The interactions in the lattice are represented by a Morse potential. The sputtering is caused by a recoiling lattice atom, so that the ion enters only into the initial collision and the model should be fairly applicable to N_2^+ bombardment. The energy taken up by dissociation would tend to make the observed yields lower than those predicted by the theory.

As predicted from Langberg's theory, the threshold and cut-in energies, in ev, are as follows:

	Threshold	Cut-in		Threshold	Cut-in
Fe–N_2^+	51.0	76	Cu–N_2^+	45.0	73
Fe–N^+	70.6	105	Cu–N^+	64.8	100
Mo–N_2^+	96.0	140	Ni–N_2^+	54.0	88
Mo–N^+	151	220	Ni–N^+	76.1	124
W–N_2^+	196	288	Cu–A^+	40.4	66
W–N^+	340	500			

It is not possible to draw meaningful straight lines through our low energy data, so that no "observed values" are quoted for comparison (it is not entirely clear whether the lack of linearity is a real effect or an apparent one due to experimental scatter). It is quite clear from the data, however, that the predicted thresholds are invariably too high (see figs. 6 through 12). This is particularly apparent in copper and nickel, for which more extensive low energy data were obtained (fig. 7); while the theoretical thresholds range from 45 to 76 ev, significant amounts of sputtering are still present at 25 ev.

The many discrepancies noted in the above discussion emphasize the need for additional theoretical work and experimental data. Existing models fail to explain many observed features of sputtering, although they take into account all of the apparently significant energy, momentum, and structural parameters of the ions and lattices involved. It is strongly suggested that the details of the interaction models are at fault, in particular the assumption of successive binary collisions. This assumption is usually justified for the representation of the large-angle deflection resulting from a series of small-angle and small-energy-transfer collisions, which is to say in the case of weak interactions. This is not a good assumption for the sputtering process. It appears, therefore, that one must seek better approximate representations of the multibody interactions involved.

THE EFFECTS OF PRESSURE, TEMPERATURE, AND BEAM INTENSITY

An attempt was made at controlling independently the pressure in the target area, the target temperature, and the beam density. In order to achieve good control over sizable ranges of these parameters, one would need excess pumping capacity and an independent means of heating or cooling the targets. Modifications of the apparatus are now under way to meet these needs. In the meantime, however, it was found possible to obtain a certain amount of data over more limited ranges of the parameters in question.

The target temperature was varied between 40° and 120° C by changing the total incident beam current, at the same time keeping the beam density as constant as possible by adjusting the focusing. Iron is the only metal for which a temperature dependence of the sputtering yield was found. The yield has a constant value from 120° down to 80° C, then drops to 80 percent of this value at 40° C. The values presented in figure 10 correspond to the constant-value range between 80° and 120° C.

The results obtained on pressure effects are more easily interpretable. The nitrogen pressure in the target chamber during bombardment was generally 9×10^{-6} mm Hg, while the partial pressure of other gases was 4×10^{-7} mm Hg, as estimated from the residual pressure before the beam was turned on. The significance of this can be better understood in terms of the number of collisions per second with the targets. These are shown in the following table, where it has been assumed that oxygen constituted the bulk of the residual gases.

	Collisions cm^{-2} sec^{-1}
Beam particles at 250 $\mu a/cm^2$	1.6×10^{15}
Target chamber N_2	
(a) av. pressure $=9\times10^{-6}$ mm Hg	3.6×10^{15}
(b) min. pressure $=6\times10^{-6}$ mm Hg	2.4×10^{15}
(c) max. pressure $=6\times10^{-5}$ mm Hg	2.4×10^{16}
Target chamber O_2	
O_2 pressure $=4\times10^{-7}$ mm Hg	1.6×10^{1}

At the usual operating pressures, the number of beam and ambient nitrogen collisions per second with the target were of the same order while the collision number for oxygen was an order of magnitude lower. For sputtering yields $\gtrsim 1$ atom/ion, it is thus improbable that oxidation of targets introduced any significant errors, even in the case of nickel (the most likely of the metals investigated to form oxide coatings).

The pressure was varied over an order of magnitude (see above table) both by choking the pumps and by introducing controlled oxygen and nitrogen leaks. For the five metals investigated, the yields are about 10 percent lower at 6×10^{-5} than at 6×10^{-6} mm Hg. This is quite clear even in the presence of the 15-percent scatter in the data, but no differences can be seen between the several methods of varying the pressure. The lowering observed is the same as has been reported by Yonts, Normand, and Harrison (ref. 1) in the same pressure range.

It is instructive at this point to examine the Cu–A^+ data shown in figure 6. In all cases in which the data are lower than those of the present experiment, the pressure was either known or suspected to be above 1×10^{-4} mm Hg. The agreement between the present data and that of Wehner is remarkable, as the argon pressure in Wehner's apparatus was above 10^{-3} mm Hg (ref. 12). The bombarding current densities used by Wehner, however, were 5 to 12 ma/cm^2, as compared with 0.2 to 0.5 ma/cm^2 in the present experiment. These observations strongly suggest that, in the range 10^{-6} to 10^{-3} mm Hg, the lowering of yields is due to some surface contamination process such as adsorption. Between 10^{-3} and 10^{-2} mm Hg, mean free paths become comparable to apparatus dimensions, and back-diffusion of sputtered atoms plays an increasingly important part in lowering the observed sputtering yields. The number of collisions per second (with the target) of background argon was an order of magnitude larger than that of A^+ collisions with the target in Wehner's apparatus. It would appear, then, that the elimination of adsorption effects may be due to local heating of the targets resulting from the relatively high beam density.

It is clear from the above discussion that further experimentation is needed to separate clearly the effects of pressure, temperature, and beam density. It appears from the present data that no further variation with pressure will occur below about 10^{-6} mm Hg, but the beam density could not be varied over a sufficient range to check on the effect of remaining adsorptions at these pressures. It must, in any case, be borne in mind that the effects of local heating (high beam density) can be twofold: first, adsorbed gases can be driven off; and second, local melting and evaporation may tend to dominate the sputtering process.

SUMMARY OF RESULTS

The application of high-intensity, high-resolution ion-beam techniques to very low energies (20 ev to 8 kev) has proved feasible and highly successful in obtaining heretofore unavailable data under closely controlled experimental conditions. The first results obtained with the Ames 8 kv accelerator are sputtering yield curves of five metals (Cu, Ni, Fe, Mo, and W) under N^+ and N_2^+ bombardment. These curves follow the general pattern of a rapid rise from very low yields around 25 ev to a plateau around 3 kev. They exhibit, in addition, a number of noteworthy features, summarized below together with the main derivative conclusions.

1. Similarities might be expected between Cu and Ni as they both form fcc crystals and have similar atomic weights and atomic heats of sublimation. The only significant similarity found, however, was a slight downward trend appearing in the Cu–N^+ and Ni–N^+ yields above approximately 6 kev.

2. The ratio of 45° to normal incidence yields is lower in Cu than in Ni. This may be due to the difference in their electronic configurations. Small angular dependencies of yields have also been reported for the noble metals, Ag, Pt, and Au, which are electronically similar to Cu. The effect of electronic configuration is not understood: it should affect total yields, but not ratios of 45° to normal incidence yields.

3. The ratios of 45° to normal incidence yields are somewhat higher for the bcc than for the fcc metals, but they are much smaller than those reported for Hg^+ bombardment. Data on additional bombarding ions are needed to determine whether this is simply a mass and size effect.

4. The sputtering produced by an N_2^+ ion is generally not the same as that of 2 N^+ ions with the same total energy, although N_2^+ should dissociate on impact.

(a) At normal incidence, the N_2^+ and $2N^+$ yields coincide for the fcc metals examined (Cu, Ni), but for the others (Fe, Mo, W), the $2N^+$ yields are too low at low energies and too high at high energies.

(b) At 45° incidence, the $2N^+$ yields are too low at low energies and are either lower than or equal to the N_2^+ yields at higher energies.

5. In spite of the expected similarity between N_2^+ and N^+ bombardment, no correlation of yields is obtained, nor are the discrepancies of item 4 above resolved, by attempts at normalizing bombarding energies with combinations of energy transfer factors, momentum transfer factors, and heats of sublimation.

6. Yields in the threshold region are considerably higher than have been predicted on the basis of energy transfer to the lattice, heat of sublimation, crystal structure, and numbers and types of lattice bonds.

The principal summarizing conclusion drawn from the data is that classical models using binary collisions are inadequate to describe the sputtering process. This is brought out particularly by the dominance of the effect of electronic configuration over that of crystal structure (item 2) and the absence of simple correlations between N_2^+ and $2N^+$ yields (items 4 and 5). There are, in addition, some observations which may be of practical importance. In particular, the yields in the threshold region are higher than expected, oblique incidence yields are higher than normal incidence yields, and yields are higher at low pressures or at locally high temperatures.

AMES RESEARCH CENTER
NATIONAL AERONAUTICS AND SPACE ADMINISTRATION
MOFFETT FIELD, CALIF., *Feb. 16, 1961*

REFERENCES

1. Yonts, O. C., Normand, C. E., and Harrison, Don E., Jr.: High-Energy Sputtering. Jour. Appl. Phys., vol. 31, no. 3, Mar. 1960, pp. 447–450.
2. Wehner, G. K.: Sputtering by Ion Bombardment. Advances in Electronics and Electron Physics, vol. VII, Academic Press, Inc., New York, 1955, pp. 239–298.
3. O'Briain, Cormac D., Lindner, Amelie, and Moore, Walter J.: Sputtering of Silver by Hydrogen Ions. Jour. Chem. Phys., vol. 29, no. 1, July 1958, pp. 3–7.
4. Rol, P. K., Fluit, J. M., and Kistemaker, J.: Sputtering of Copper by Ion-Bombardment in the Energy Range of 5–25 kev. Proc. International Symposium on Isotope Separation, North-Holland Pub. Co., Amsterdam, 1958, pp. 657–662.
5. Gronlund, Finn, and Moore, Walter J.: Sputtering of Silver by Light Ions With Energies From 2 to 12 kev. Jour. Chem. Phys., vol. 32, no. 5, May 1960, pp. 1540–1545.
6. Pitkin, E. T., MacGregor, M. A., Salemme, V. J., and Bierce, R.: Investigation of the Interaction of High Velocity Ions With Metallic Surfaces. Final Rep. 25022, ARL–TR–60–299, The Marquardt Corp., June 1960.
7. Bradley, R. C.: Sputtering of Alkali Atoms by Inert Gas Ions of Low Energy. Phys. Rev., vol. 93, no. 4, Feb. 15, 1954, pp. 719–728.
8. Wehner, G. K.: Controlled Sputtering of Metals by Low-Energy Hg Ions. Phys. Rev., vol. 102, no. 3, May 1, 1956, pp. 690–704.
9. Wehner, G. K.: Sputtering Yields for Normally Incident Hg^+-Ion Bombardment at Low Ion Energy. Phys. Rev., vol. 108, no. 1, Oct. 1, 1957, pp. 35–45.
10. Wehner, G. K.: Low-Energy Sputtering Yields in Hg. Phys. Rev., vol. 112, no. 4, Nov. 15, 1958, pp. 1120–1124.
11. Laegreid, N., Wehner, G., and Meckel, B.: Sputtering Yield of Germanium in Rare Gases. Jour. Appl. Phys., vol. 30, no. 3, Mar. 1959, pp. 374–377.
12. Wehner, G. K.: Annual Report on Sputtering Yields. Rep. 1902, General Mills, Inc., May 31, 1959.
13. Wehner, G. K.: Velocities of Sputtered Atoms. Phys. Rev., vol. 114, no. 5, June 1, 1959, pp. 1270–1272.
14. Wehner, G. K., and Rosenberg, D.: Angular Distribution of Sputtered Material. Jour. Appl. Phys., vol. 31, no. 1, Jan. 1960, pp. 177–179.
15. Keywell, F.: Measurements and Collision–Radiation Damage Theory of High Vacuum Sputtering. Phys. Rev., vol. 97, no. 6, Mar. 15, 1955, pp. 1611–1619.
16. Harrison, Don E., Jr.: Theory of the Sputtering Process. Phys. Rev., vol. 102, no. 6, June 15, 1956, pp. 1473–1480.
17. Harrison, Don E., Jr.: Extended Theory of Sputtering. Jour. Chem. Phys., vol. 32, no. 5, May 1960, pp. 1336–1341.
18. Henschke, E. B.: New Collision Theory of Cathode Sputtering of Metals at Low Ion Energies. Phys. Rev., vol. 106, no. 4, May 15, 1957, pp. 737–753.
19. Langberg, E.: Analysis of Low-Energy Sputtering. Phys. Rev., vol. 111, no. 1, July 1, 1958, pp. 91–97.
20. Peterson, J. R., Cook, C. J., and Heinz, O.: Beam Extraction From an RF Ion Source. SRI Tech. Rep. 720–1, Stanford Research Inst., July 15, 1960.
21. Guntherschulze, A.: Kathodenzerstaubung bei sehr geringen gasdrucken. (Sputtering of a Large Number of Metals in a Hydrogen Glow Discharge) Z. Phys., vol. 38, 1926, p. 575.
22. Penning, F. M., and Moubis, J. H. A.: Cathode Sputtering in a Magnetic Field. Proc. Kon. Ned. Akad. v. Wetensch., Amsterdam, vol. 43, 1940, pp. 41-56.

U.S. GOVERNMENT PRINTING OFFICE: 1961